

CATHODO- AND PHOTO-LUMINESCENCE OF ERBIUM IONS IN NANO-CRYSTALLINE SILICON: MECHANISM OF EXCITATION ENERGY TRANSFER

dedicated to Stanford R. Ovshinsky on the occasion of his 80th anniversary

R. Plugaru, J. Piqueras, E. Nogales, B. Méndez, J. A. García^a, T. J. Tate^b

Universidad Complutense de Madrid, Facultad de Ciencias Físicas, Departamento de Física de Materiales, 28040 Madrid, Spain

^aUniversidad del País Vasco, Departamento de Física Aplicada II, Lejona, Vizcaya, Spain

^bDepartment of Electrical and Electronic Engineering, Imperial College of Science and Technology, London, United Kingdom

The processes of the characteristic radiative transition of Er³⁺ ions involved in optically active centers in nano-crystalline silicon have been studied by photo-luminescence (PL) and cathodo-luminescence (CL). Infrared emission is observed in cathodo-luminescence and in photoluminescence spectrum excited with photons of 488 nm. The maximum intensity at 1540 nm was obtained under photons excitation and is about ten times higher in nanocrystalline silicon doped with Er and O than in Er doped crystalline silicon.

(Received October 29, 2002; accepted October 31, 2002)

Keywords: Nano-crystalline silicon, Cathodo-luminescence, Photo-luminescence, Erbium ion

1. Introduction

Optical activity of erbium in silicon-based materials has been widely investigated due to the interest in silicon integrated light emitting devices fabrication [1, 2]. The indirect band gap and low quantum efficiency of silicon makes this material not suitable for optical applications. Among the various processes investigated in view of increasing the silicon luminescence efficiency, doping with rare earth elements has been considered as a promising possibility [3]. The main characteristics of the luminescence from rare earth atoms are the sharp and temperature stable emission, which arise from 4f-4f intraionic radiative transitions. Of particular interest is the infrared Er³⁺ ion emission at 1.54 μm , which correspond to a transition between the first excited state and the ground state, $^4I_{13/2}$ - $^4I_{15/2}$, and is a standard wavelength in optical telecommunication. Other transitions, extending the luminescence emission from visible to near infrared region could take place, depending on the host matrix and on the structure of Er-related optically active centers [4, 5, 6]. The emission process is independent on the matrix in which the rare earth ions are incorporated, but the excitation mechanism is characteristic of each host material. Energy transfer efficiency correlates with the structure of the semiconductor. Amorphous silicon shows a wide number of defect states contributing to the excitation process [7, 8] while in the host matrix containing silicon nanocrystallites, excitation process of Er occurs through recombination of carriers photogenerated in the nanocrystalline structures. The intensity of infrared emission increases in the presence of nanocrystallites, and strongly correlates with their size [9, 10].

In crystalline silicon, energy transfer involves electron-hole pair recombination, hot electron excitation, or defect Auger recombination of excitons [11, 12]. The efficiency of the excitation process increases in the presence of codoping elements, among the most commonly used is O, which increase the negative field around the Er ions and make possible the internal transitions that are normally forbidden. The efficiency of energy transfer is increased if high symmetry Er-O centers are formed [13, 14, 15].

In this work we investigate the mechanisms of erbium excitation in nano-crystalline silicon when Er complexes involving Er-O, Er-Si and Er-Er bonds are formed under thermal treatments. The energy transfer from matrix through recombination of electron-hole pairs, as well as defect-related Auger excitation and phonon assisted energy transfer are reported as mechanisms assisting the luminescent emission of erbium. Visible to infrared cathodo- and photo-luminescence emission has been obtained and its correlation with specific Er centers has been analyzed.

2. Experiment

Amorphous silicon films with a thickness of about 2 μm were obtained by low-pressure chemical vapour deposition on p-type (100) silicon wafers at 570 $^{\circ}\text{C}$ and a pressure of 0.4 torr. The films were implanted with 200 keV ^{166}Er ions at doses of 5×10^{15} ions/ cm^2 . Some of the amorphous silicon layers were coimplanted with 200 keV Er ions and 40 keV ^{16}O ions at doses of 5×10^{15} and 10^{16} ions/ cm^2 respectively.

The implanted samples were annealed at temperatures of 600 $^{\circ}\text{C}$, 750 $^{\circ}\text{C}$ and 900 $^{\circ}\text{C}$ respectively for half hour in nitrogen atmosphere and slowly cooled down to room temperature.

In order to understand the structure and luminescence emission mechanism of Er-O optically active centers formed in the implanted samples, two sets of erbium oxide samples were investigated. Erbium oxide was grown on amorphous and crystalline silicon substrates by erbium vapour deposition and treatments at 950 $^{\circ}\text{C}$ during 1 hour in oxygen atmosphere.

X-ray diffraction measurements were performed at grazing angle. All the samples were observed in the CL mode of operation in a Hitachi S2500 SEM in the temperature range 80-300 K and at accelerating voltage of 25 kV. For the detection of visible light a Hamamatsu R-928 photomultiplier was used while for the near infrared light a cooled ADC germanium detector was employed. CL spectra were recorded by using an Oriel 78215 computer controlled monochromator or, in the visible range, with a CCD camera with a built-in spectrograph (Hamamatsu PMA-11).

The PL measurements were performed with a CD-900 spectrometer system from Edinburgh Instruments. The samples were cooled at 10 K in a closed-cycle helium cryostat. The excitation sources were a He-Cd laser at 325 nm and excitation power of 50 mW and an Ar-ion laser at 488 nm with an excitation power of 20 mW.

3. Er centers in nc-Si implanted with Er and Er and O

Silicon layers used in the experiment were obtained by LPCVD at temperature and pressure conditions leading to an initial amorphous structure of the deposited layers. Following implantation with Er and Er and O, annealing treatments in the temperature range 600-900 $^{\circ}\text{C}$ were performed for both amorphous and crystalline silicon samples used as reference.

Low temperature annealing favoured a rather uniform distribution of Er in the host matrix. XRD spectrum of a-Si: Er, O layer shows a well formed Er-O phase at this temperature with Er_2O_3 structure, as well as the presence of an Er-Si compound whose best fit structure is Er_5Si_3 . In a solid host matrix in which O and Er are present, Er getter O atoms forming Er-O complexes with various structures, ErO_4 , ErO_6 or Er_2O_3 /5,7,16/. The crystal field splitting of the 4f states is influenced by the presence of oxygen in various coordination configurations. Six fold O coordination to Er similar to Er_2O_3 complex was suggested to be formed at low temperature annealing, while different types of Er-Si clusters seem to be characteristic for treatments at high temperatures [5, 7].

Silicon nanostructures could not be detected in a-Si: Er, O samples treated at 600 $^{\circ}\text{C}$ and, even at 900 $^{\circ}\text{C}$ the nanostructures formed seem to be under the detection of the XRD method. While the recrystallization of a-Si layer in the samples co-implanted with oxygen was very poor, the crystalline silicon (111) oriented phase is well developed in the samples implanted only with Er, after annealing at 900 $^{\circ}\text{C}$. High temperature treatment seems to favour the formation of Er-Si complexes and in fact Er_5Si_3 precipitates were present in the XRD spectrum of all implanted layers after the high temperature annealing. In the secondary electron mode of the SEM, the surface of the samples appears as a flat and homogeneous background, with a random distributed dots like structure, which is

correlated with the occurrence of the erbium precipitates. The dot size and density increase with annealing temperature and their average size was around 10 μm .

Er segregation was reported to take place during epitaxial growth of Er-doped silicon and a structure resembling Er_3Si_5 was proposed for the Er precipitates. The critical implantation dose reported for Er precipitation was around 2×10^{14} ions/ cm^2 [17]. In crystalline silicon, Er precipitation appears at an implantation concentration of 1.2×10^{14} ions/ cm^2 and 900 °C temperature of annealing process [18] with formation of platelet precipitates phase similar to ErSi_2 . The platelet diameter was about 100-300 Å. In our experiment, the best fit for the precipitate structure observed in XRD spectra of the implanted layers and crystalline silicon was Er_3Si_5 , for an implantation dose of 5×10^{15} Er ions/ cm^2 and 10^{16} O ions/ cm^2 . From TRIM simulation we found that the maximum concentration of Er was 10^{21} ions/ cm^3 appears at a depth penetration of 150 nm. The amorphous silicon structure, as well as the presence of O allowed a larger amount of Er incorporation before the precipitation process appears.

A structure of extended precipitates involving several Er atoms and possibly oxygen gives rise to a clear emission band in the violet-blue region, observed in CL and mainly in PL spectra.

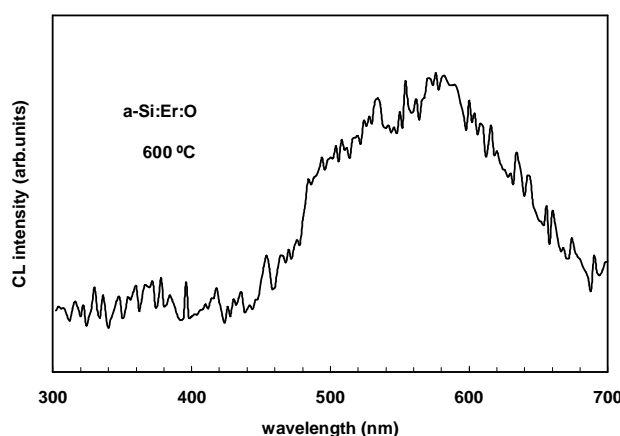


Fig. 1. Cathodo-luminescence spectrum of a-Si:Er, O implanted layer. Annealing at 600 °C favours the formation of erbium oxide complexes. The luminescence emission in the green-red region is associated with these complexes.

4. CL and PL in the visible range

Luminescence emission of the samples has been investigated by cathodo-luminescence and photo-luminescence. The differences in the excitation power and selectivity of the two methods enabled us to observe the contribution of various types of Er complexes in the emission spectra. Fig. 1 shows the CL spectrum of the a-Si:Er, O sample treated at 600 °C. The dominant emission is situated in the green-red region, with a broad peak centered at 580 nm. The PL spectrum of the sample, excited with photons of 325 nm wavelength, shows emission bands with a step-like structure in the violet-blue region at 360-370 nm and a broad band showing two components at 420 nm and 450 nm, respectively (Fig. 2). It appears that, high energy electrons and the 325 nm photons, give a selective activation of luminescent transitions associated with optically active Er centers formed at 600 °C in the a-Si matrix.

Visible bands at 550 nm and 655-675 nm corresponding to Er^{3+} intra-shell transitions appear in the CL spectrum of pure erbium oxide powder, Er_2O_3 , are shown in Fig. 3, [19]. The same strong CL green emission as well as a less intense red band could be observed when an erbium oxide layer was grown on crystalline silicon substrate, c-Si/Er/O, Fig. 3 [19]. Characteristic emission bands of Er^{3+} ion in the visible region were reported at 530, 554 and 580 nm, related to Er_2O_3 phase formation in erbium doped zinc telluride glasses [20]. The correlation of the spectral emission and the presence

of erbium oxide phase in the sample doped with Er and codoped with O after treatment at 600 °C confirm that the local microstructure around the Er^{3+} is similar to the environment in the E_2O_3 .

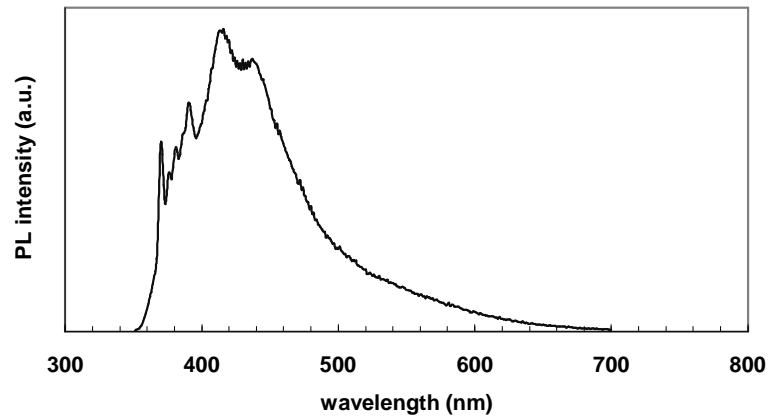


Fig. 2. Photoluminescence spectrum of an a-Si:Er, O implanted layer, annealed at 600 °C. Excitation with photons of 325 nm wavelength evidence luminescence emission associated with erbium precipitates. The step-like peaks structure in the region 370-390 nm shows the existence of phonons assisted transitions.

The emission from the optically active centers formed in the a-Si host cover however a wider spectral region than that of erbium oxide and the two mentioned bands, at 550 nm and 655-675 nm are present but not well resolved in the spectrum of Fig. 1. A tentative explanation for excitation of visible luminescence emission, showed that the recombination of electron beam generated e-h pairs through Er^{3+} ions, and the resonant photons energy transfer can be considered [6]. The energy-level diagram of Er^{3+} is shown in Fig. 4. In our experiment, green-red emission could not be observed under photon excitation. Resonant energy transfer takes place when 325 nm wavelength photons were used causing excitation of violet-blue luminescence (Fig. 2).

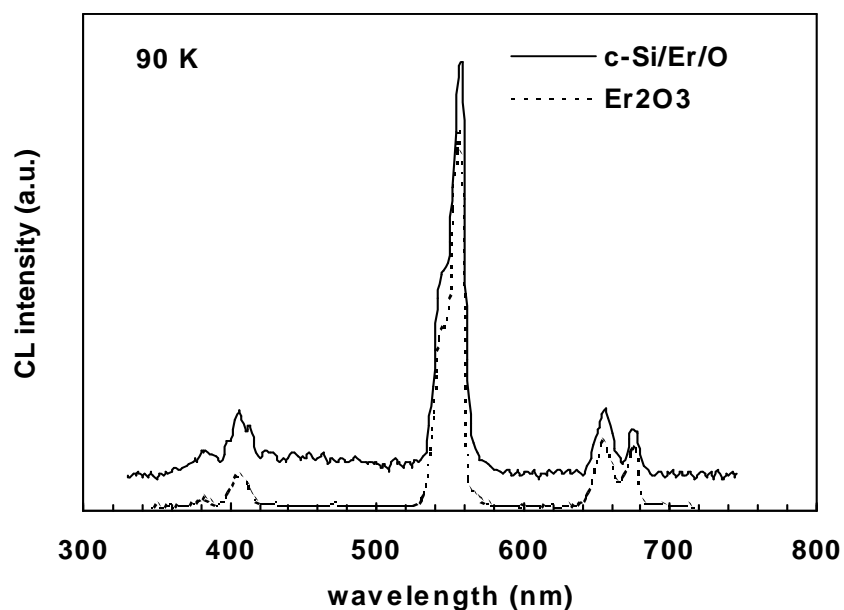


Fig. 3. Cathodo-luminescence spectra of erbium oxide powder and of erbium-oxide layer grown on a crystalline silicon substrate. Intense green and relatively lower red emission, characteristic of Er^{3+} intrashell transitions were observed at 90 K.

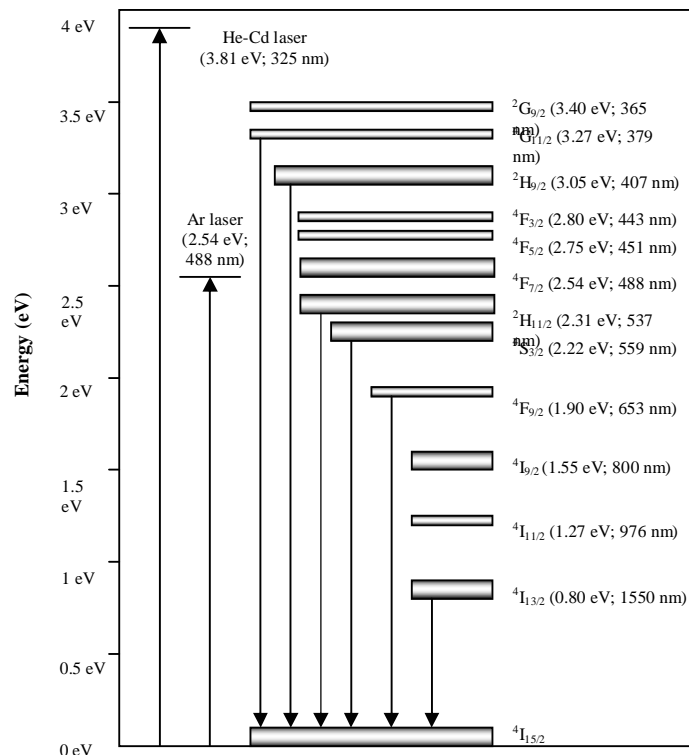


Fig. 4. Energy level diagram of Er^{3+} ion and the intrashell transitions observed by excitation with electrons beam and photons of 325 nm (He-Cd laser) and of 488 nm (Ar-ion laser).

A dominant PL emission in the violet-blue region is observed in all the spectra of the samples treated at 900 °C, in which the occurrence of Er-Er structures forming Er_5Si_3 precipitates was detected. A CL local spectrum recorded on a precipitate structure shows a sharp emission peak at 300-400 nm. Bright spots were observed in the CL images to correspond with the precipitates. The contribution of the precipitates emission is clearly observed in the CL spectrum of Fig. 5. The emission spectrum of a-Si:Er, O sample shows an intense emission band peaked at about 360-370 nm. Other less intense bands at 410, 470 nm are observed. The green band corresponding to Er_2O_3 appears with a very weak intensity [21]. The PL spectrum of the a-Si:Er sample is shown in Fig. 6. A step-like structure is observed in the region 350-370 nm at the high energy side of a broad band peaked at about 420-430 nm. The multi-peak emission is also present in the c-Si: Er implanted sample but not so well resolved as in the spectrum of Fig. 2. The successive transitions induced by excitation with photons of 325 nm show the existence of phonons assisted radiative process. The excitation energy transfer from the matrix to Er^{3+} ion takes place through a nonradiative process, involving the Er_5Si_3 precipitates.

5. CL and PL in the infrared range

The selective character of PL excitation is also revealed in the excitation processes of infrared emission. The Er^{3+} intra shell transitions involving first excited state and the ground state (${}^4\text{I}_{15/2}$ - ${}^4\text{I}_{13/2}$ in Fig. 4) were observed under excitation with photons of 488 nm, but not with 325 nm photons. The near infrared PL spectrum of the a-Si:Er, O sample treated at 600 °C is shown in Fig. 7. A complex peak structure, with the intense bands situated at: 1300, 1400, 1540, 1610 and 1630 nm is observed. The origin of the different emission bands is related to Er_2O_3 phase formation in the sample, as well as to other oxides structure and oxygen related defects present in a-Si matrix after this annealing

treatment. The oxygen occupies optimum position around the erbium, the interaction of Er electrons with the surrounding crystalline field determining the splitting of the 1540 nm emission.

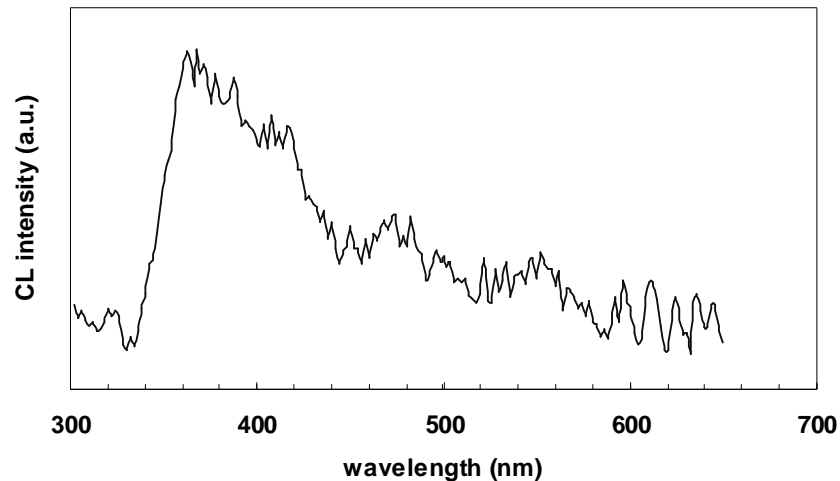


Fig. 5. Cathodo-luminescence spectrum of a-Si: Er, O implanted layer annealed at 900 °C. Intense luminescence emission observed in the violet – blue region is associated with the presence of erbium precipitates.

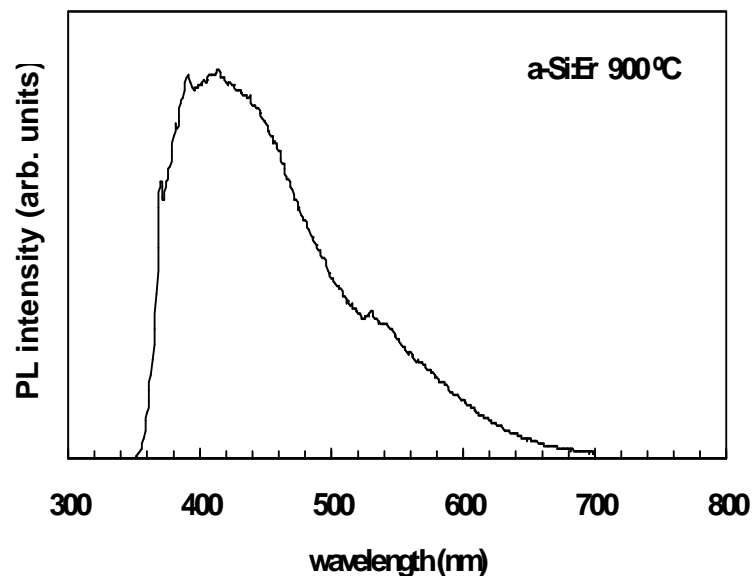


Fig. 6. Visible photo-luminescence emission from a-Si:Er implanted layer treated at 900 °C under excitation with 325 nm photons.

Stark splitting of the Er^{3+} peaks in the region 1460-1610 has been reported [7]. It could be considered that, the peaks observed in the region 1540-1610 nm result from transitions involving the fine structure of Er^{3+} levels, appearing in a suitable crystalline environment. The relatively intense emission band at about 1310 nm appears related to an Er-O defect complex. The broad band situated at 1250-1300 nm was observed in the CL spectra of erbium oxides grown on different crystalline substrates and has been attributed to a defect involving oxygen [22]. A poorly resolved step-like peaks structure can be observed in the region 1100-1300 nm region in the spectrum of the Fig. 7, and could be related to phonon assisted radiative transitions, similar to the process observed in the violet region. Infrared PL emission from the a-Si:Er, O implanted layer treated at 900 °C shows a sharp emission

peak centered at 1540 nm as in Fig. 8. The structure in which the Er^{3+} ion is involved seems to be different of the Er-O complex formed at 600 °C annealing. The emission intensity is higher than in other samples, showing a strong energy transfer from the matrix (Fig. 9). The emission from this sample could be excited with photons of both, 325 nm and 488 nm wavelengths used (see Fig. 8). The less selective character of electron beam excitation results in a very low emission in the infrared region. Fig. 10 shows the CL spectrum of the same sample. Considering that the optimum crystalline field around the Er^{3+} was obtained in the Er_2O_3 complex structure, whose maximum emission appears in the sample treated at 600 °C, it seems that the higher intensity of the emission from the sample treated at 900 °C is determined by changes of the a-Si matrix and the presence of silicon nanostructures possibly formed at this temperature.

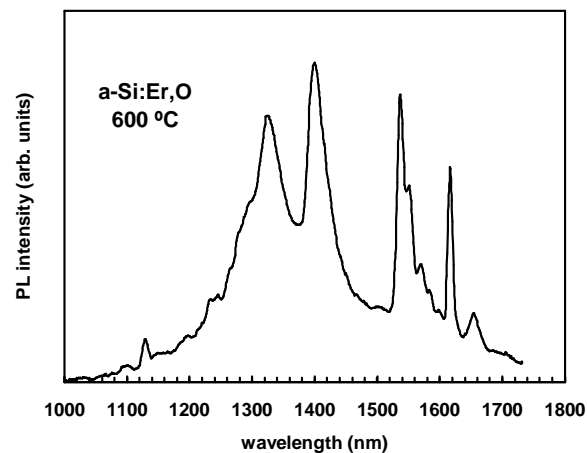


Fig. 7. Complex bands structure in the infrared region from a-Si:Er, O layer treated at 600 °C. Stark splitting observed under excitation with photons of 488 nm wavelength.

6. Mechanism of energy transfer

The selective excitation of luminescence emission of Er^{3+} ions is related to the presence of optically active centers formed at each particular temperature of annealing. It is well known that an ionic environment tends towards a more efficient lifting of the f-f dipole forbidden transition in isolated ion than in a covalent one.

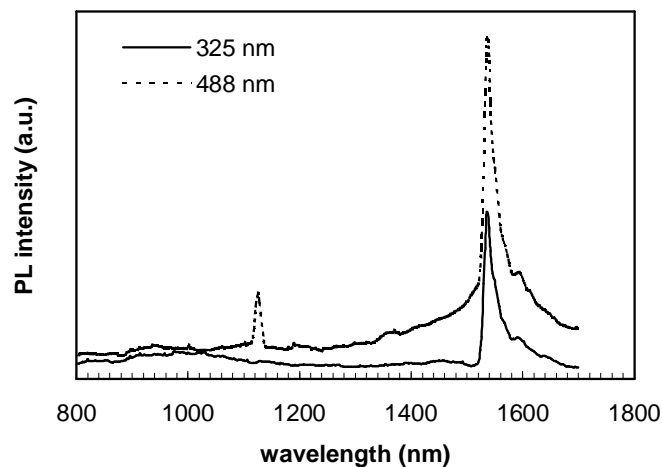


Fig. 8. Photo-luminescence emission in infrared region from a-Si:Er, O implanted layer annealed at 900 °C. Sharp intrashell transition of Er^{3+} at 1540 nm appears under both 325 nm and 488 nm photons excitation.

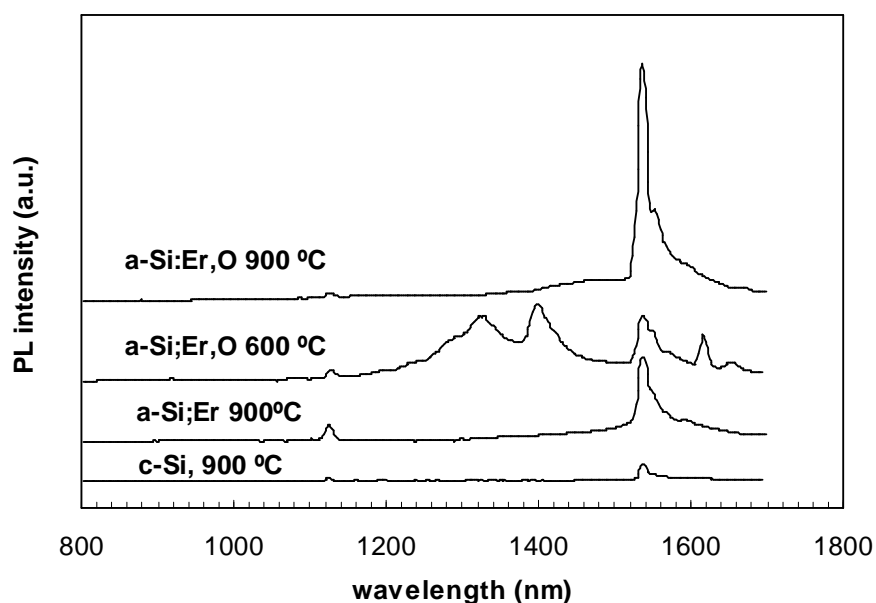


Fig. 9. Infrared PL spectra from the implanted layers and implanted crystalline silicon obtained under excitation with 488 nm photons wavelength. The higher intensity of the emission was obtained in the a-Si:Er, O implanted layer treated at 900 °C.

From this point of view, erbium oxides and especially Er_2O_3 complex allowed efficient visible and infrared emission of Er^{3+} . However, the probability that one or other transition becomes active is related on the excitation energy transfer. The green-red emission in the CL spectrum of Fig. 1 was obtained under electron beam excitation, able to transfer enough energy for excitation of Er electrons from the ground to an upper f state. The less optically active structure of Er_5Si_3 gave a lower contribution and practically could not be observed in the spectrum of Fig. 1. Resonant energy transfer is requested to evidence the violet-blue emission and the process was observed under 325 nm photons excitation (Fig. 2). The de-excitation process is assisted by 47 meV energy phonons, as could be seen in the Fig. 11. Phonon- assisted de-excitation processes were reported in silicon quantum structures with the energy of acoustic and optical transverse phonons of 18.5 and 57.5 meV [23]. In our experiment, the step-like structure associated with nonradiative transitions was also observed in crystalline silicon implanted with Er in which erbium precipitates are present. This indicates that the phonon assisted radiative transitions involve the precipitates structure. The Er-Er structure, involving several erbium atoms and probably oxygen, seems to be related to phonon assisted radiative process. Non-radiative de-excitation processes were reported for the Er-Si system [12, 19].

The resonant energy transfer could be involved in the infrared region where the 1540 nm peak appears under 488 nm photons excitation. However, in the case of the a-Si:Er, O sample, the infrared band is also observed by excitation with 325 nm and by cathodoluminescence (Fig. 8). High efficiency of the Er^{3+} emission in this structure is also revealed by the high emission intensity. It appears ten times higher relative to the emission in the crystalline Er^{3+} implanted sample. This suggest that the nanocrystalline silicon structures formed in the matrix could increase the energy transfer efficiency [9, 10]. Anyhow, the Stark splitting observed in the infrared spectrum, shown in Fig. 7, of the same sample treated at 600 °C does not appear, indicating a different structure in the Er crystalline environment.

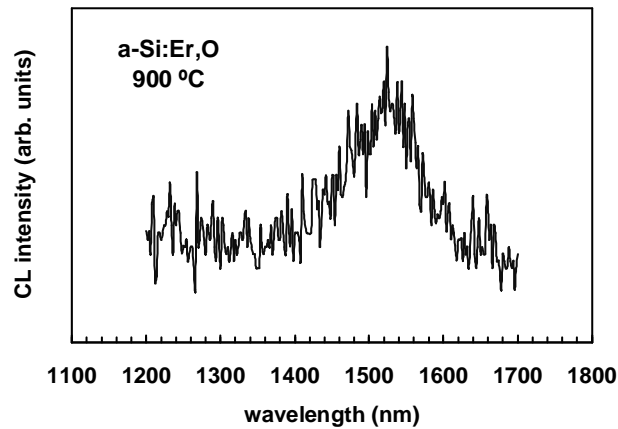


Fig. 10. Cathodoluminescence emission in the infrared region from a-Si, Er, O layer annealed at 900 °C.

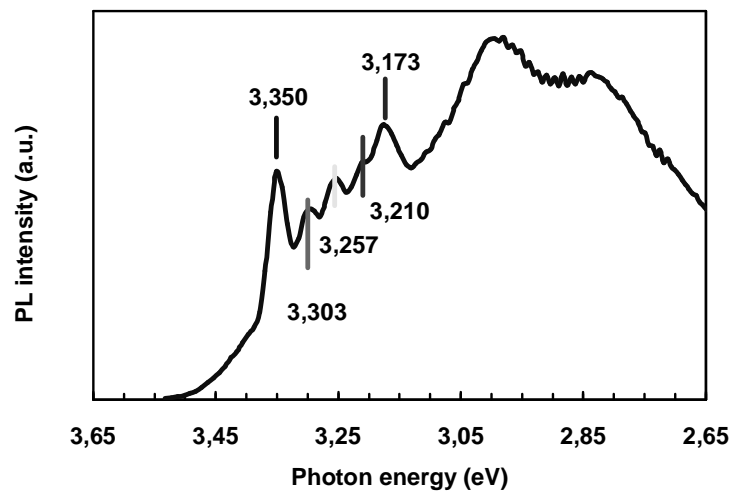


Fig. 11. Phonon assisted de-excitation process involving phonons of 47 meV energy. The resonant excitation of a-Si:Er,O implanted layer, treated at 600 °C was obtained under excitation with photons of 325 nm wavelength.

7. Conclusions

The characteristics of Er^{3+} intra-ionic 4f radiative transitions were investigated by considering the Er-Si and Er-O complexes formed in crystalline and amorphous silicon matrix.

Luminescence emission in the visible and infrared regions was obtained by electron beam excitation in the SEM and by excitation with photons of He-Cd (325 nm) laser and Ar-ion (488 nm) respectively. The selective character of photons excitation, was revealed by the excitation of photoluminescence in the visible region under photons with 325 nm wavelength and in the near infrared region when photons of 488 nm wavelength were used. Electron beam irradiation favours mainly the luminescence emission in the visible range.

The transfer of excitation energy from the host matrix to the Er ions takes place through mechanisms involving generated carriers when Er-O complexes are present, and through phonon-assisted processes, when Er precipitates are formed. In the latter case, phonon assisted radiative transitions were revealed in the violet region of the photoluminescence spectra under resonant excitation with 325 nm wavelength photons.

The resonant excitation of the infrared emission band at 1540 nm was observed under excitation with photons of 488 nm wavelength.

Acknowledgments

This work was supported by MCYT (Project MAT2000-2119). R.P. acknowledges MECD for the research grant SB 2000-0164.

References

- [1] S. Lombardo, S. U. Campisano, G. N. van den Hoven, A. Polman, *J. Appl. Phys.* **77**, 6504 (1995).
- [2] G. Z. Ran, Y. Chen, W. C. Qin, J. S. Fu, Z. C. Ma, W. H. Zong, H. Lu, J. Qin, G. G. Qin, *J. Appl. Phys.* **90**, 5835 (2001).
- [3] A. Polman, *J. Appl. Phys.* **82**, 1 (1997).
- [4] M. Markmann, A. Sticht, F. Bobe, G. Zandler, K. Brunner, G. Abstreiter, E. Müller, *J. Appl. Phys.* **91**, 9764 (2002).
- [5] H. Przybylinska, W. Jantsch, Yu. Suprun-Belevitch, M. Stepikhova, L. Palmetshofer, G. Hendorfer, A. Kozanecki, R. J. Wilson, B. J. Sealy, *Phys. Rev. B* **54**, 2532 (1996).
- [6] A. R. Zanatta, C. T. M. Ribeiro, U. Jahn, *Appl. Phys. Lett.* **79**, 488 (2001).
- [7] Aldabergenova, H. P. Strunk, P. C. Taylor, A. A. Andreev, *J. Appl. Phys.* **90**, 2773 (2001).
- [8] I. Yassievich, M. Bresler, O. Gusev, *J. Non-Cryst. Solids* **226**, 192 (1998).
- [9] P. G. Kik, M. L. Brongersma, A. Polman, *Appl. Phys. Lett.* **76**, 2325 (2000).
- [10] M. Fujii, M. Yoshida, S. Hayashi, K. Yamamoto, *J. Appl. Phys.* **84**, 4525 (1998).
- [11] F. Priolo, G. Franzò, S. Coffa, A. Carnera, *Phys. Rev. B* **57**, 4443 (1998).
- [12] G. Franzò, F. Priolo, S. Coffa, *J. of Lumin.* **80**, 19(1999).
- [13] J. Michel, J. L. Benton, R. F. Ferrante, D. C. Jacobson, D. J. Eaglesham, E. A. Fitzgerald, Y. H. Xie, J. M. Poate, L. C. Kimerling, *J. Appl. Phys.* **70**, 2672 (1991).
- [14] K. Nakashima, O. Eryu, H. Akiyama, Y. Maeda, H. Ebisu, *Nucl. Instrum. Methods Phys. Res. B* **175**, 208 (2001).
- [15] D. L. Adler, D. C. Jacobson, D. J. Eaglesham, M. A. Marcus, J. L. Benton, J. M. Poate, P. H. Citrin, *Appl. Phys. Lett.* **61**, 2181 (1992).
- [16] P. H. Citrin, P. A. Northrup, R. Birkhahn, A. J. Steckl, *Appl. Phys. Lett.* **76**, 2865 (2000).
- [17] R. Serna, M. Lohmeier, P. M. Zagwijn, E. Vlieg, A. Polman, *Appl. Phys. Lett.* **66**, 1385 (1995).
- [18] D. J. Eaglesham, J. Michel, E. A. Fitzgerald, D. C. Jacobson, J. M. Poate, J. L. Benton, A. Polman, Y. H. Xie, L. C. Kimerling, *Appl. Phys. Lett.* **58**, 2797 (1991).
- [19] E. Nogales, B. Méndez, J. Piqueras, R. Plugaru, A. Coraci, J. A. García, *J. Phys D: Appl. Phys.* **35**, 295 (2002)
- [20] N. Jaba, A. Kanoun, H. Mejiri, A. Selmi, S. Alaya, H. Maaref, *J. Phys.: Condens. Matter* **12**, 4523 (2000).
- [21] R. Plugaru, B. Mendez, J. Piqueras, T. Tate, EDS 2002 Conference (Italy), accepted for publication in *J. Phys. Cond. Matter*.
- [22] E. Nogales, B. Mendez, J. Piqueras, R. Plugaru, J. A. Garcia, T. Tate, *Mat. Res. Simp. Proc.* **692**, H9.14.1 (2002).
- [23] Y. Kanemitsu, *J. Lumin.* **83-84**, 283 (1999).
- [24] G. Franzo, F. Priolo, S. Coffa, *J. Lumin.* **80**, 19 (1999).